SecA Folds via a Dimeric Intermediate†

Shannon M. Doyle,‡ Emory H. Braswell,‡,§ and Carolyn M. Teschke*,‡

Department of Molecular and Cell Biology and National Center for Analytical Ultracentrifugation, University of Connecticut, Storrs, Connecticut 06269-3125

Received February 8, 2000; Revised Manuscript Received June 13, 2000

ABSTRACT: Though many proteins in the cell are large and multimeric, their folding has not been extensively studied. We have chosen SecA as a folding model because it is a large, homodimeric protein (monomer molecular mass of 102 kDa) with multiple folding domains. SecA is the ATPase for the Sec-dependent preprotein translocase of many bacteria. SecA is a soluble protein that can penetrate into the membrane during preprotein translocation. Because SecA may partially unfold prior to its insertion into the membrane, studies of its stability and folding pathway are important for understanding how it functions in vivo. Kinetic folding transitions in the presence of urea were monitored using circular dichroism and tryptophan fluorescence, while equilibrium folding transitions were monitored using the same techniques as well as a fluorescent ATP analogue. The reversible equilibrium folding transition exhibited a plateau, indicating the presence of an intermediate. Based on the data presented here, we propose a three-state model, $N_2 \leftrightarrow I_2 \leftrightarrow 2U$, where the native protein unfolds to a dimeric intermediate which then dissociates into two unfolded monomers. The SecA dimer was determined to have an overall stability (ΔG) of −22.5 kcal/mol. We also investigated the stability of SecA using analytical ultracentrifugation equilibrium and velocity sedimentation, which again indicated that native or refolded SecA was a stable dimer. The rate-limiting step in the folding pathway was conversion of the dimeric intermediate to the native dimer. Unfolding of native, dimeric SecA was slow with a relaxation time in H_2O of 3.3×10^4 s. Since SecA is a stable dimer, dissociation to monomeric subunits during translocation is unlikely.

The amino acid sequence of a polypeptide determines the folding pathway and final three-dimensional structure of a protein (*1*). However, the mechanism by which the amino acid sequence directs the folding of a protein is still unknown. Determining the mechanism by which a protein folds has important implications for human health since many diseases such as Alzheimer's disease, osteogenesis imperfecta, and prion-based diseases have been linked to misfolding and aggregation of proteins (*2, 3*). In addition, the study of how a protein folds is of importance to biotechnology. Many proteins that are produced in heterologous hosts form inclusion bodies, causing the loss of that protein (*4*−*6*). If the relationship between amino acid sequence and protein folding were understood, the problems associated with protein misfolding could be more easily addressed.

Typically, protein folding studies are performed with small, single-domain proteins as models (*7*−*9*). These model systems are chosen because the folding is reversible and they give a more simplified view of folding. However, many proteins in the cell are large with multiple folding domains and subunits. Most likely, these large proteins do not follow all of the folding principles established for smaller proteins, and probably have more complex folding rules. Consequently, the study of small monomeric proteins is not sufficient for determining the folding rules of larger proteins, particularly with respect to how the amino acid sequence controls subunit−subunit interactions or interactions between domains. For example, it has been established that the folding of large proteins usually occurs with a rapid hydrophobic collapse followed by a slower second phase that often consists of an molten globule intermediate (*10*). The molten globule continues along the folding pathway through domain pairing or subunit association into an oligomer and, finally, into the native conformation (*11, 12*). With certain proteins such as P22 tailspike protein and bacterial luciferase, subunit association occurs before folding is completed (*13*−*16*). In other proteins such as aspartokinase I, homoserine dehydrogenase I, and malate dehydrogenase, each subunit is first folded and then the folded subunits associate into a larger complex (*12, 17*). Subunit association is often the rate-determining (slow) step in the folding of a large, multidomain protein (*11, 12, 18*). As a result of slow subunit association or slow folding, the protein may form aggregates instead of achieving the native conformation via the productive folding pathway.

We would like to determine how the amino acid sequence directs the processes of subunit folding and association in large multimeric proteins. We would also like to explain how these large proteins avoid kinetic traps which lead to aggregation. How large proteins avoid aggregation is a particularly interesting aspect of their folding since their size often precludes the use of molecular chaperones, such as

† This work was supported by the University of Connecticut Research Foundation. Analytical ultracentrifugation was supported by NSF Grant BIR 9318373.

* To whom correspondence should be addressed at the Department of Molecular and Cell Biology, University of Connecticut, 75 N. Eagleville Rd., U-3125, Storrs, CT 06269-3125. Tel.: 860-486-4282; Fax: 860-486-4331; E-mail: teschke@uconnvm.uconn.edu.

‡ Department of Molecular and Cell Biology.

§ National Center for Analytical Ultracentrifugation.

10.1021/bi000299y CCC: $19.00
Published on Web 08/25/2000

GroEL/S, to assist in their folding. Many labs have studied the folding of multimeric enzymes using a variety of techniques (*7, 19*−*21*). We have chosen to address these specific issues about the folding of large proteins using the SecA protein. SecA is a stable homodimer with each monomer having 901 residues (*22*). It is found in both the cytoplasmic and the membranous fractions of *Escherichia coli* where it is a necessary component of the Sec-dependent translocation pathway used by various cytosolic proteins (*23*). SecA has ATPase activity which is necessary for the translocation of preproteins across the inner membrane to the periplasmic space (*24, 25*). Each SecA monomer contains two ATP binding sites, one high affinity ($K_d = 0.13$ μM) and one low affinity ($K_d = 340$ μM) (*26, 27*). Other protein components, such as SecB (*28*), SecY, -E, and -G (*24, 29, 30*), and anionic phospholipids (*31, 32*), are also required for translocation to occur. Currently, it is believed that SecA is a dimer while associated with the membrane (*22, 33*). SecB binding to SecA has been shown to require dimeric SecA (*34*). The C-terminal domain has been tentatively identified as containing the SecA dimerization site (*35*). The C-terminal region has been shown to directly bind SecY (*36, 37*), SecB (*34*), and anionic phospholipids (*38*). The C-terminus of SecA also appears to contain a site for Zn^{2+} binding which may stabilize the SecB binding site (*39*). A 65 kDa fragment of the C-terminal domain and also a 30 kDa portion of the amino-terminal domain have been shown to be protease resistant (*40, 41*).

In addition to serving as a model for the folding of a large protein, the folding of SecA is of interest, because in the normal translocase cycle, SecA may partially unfold, possibly to a molten globule-like conformation (*41*). This unfolding has been postulated to occur when SecA inserts itself into the inner membrane as part of the preprotein translocation process (*42*−*44*). With this insertion, SecA brings ∼20−30 amino acids of the preprotein across the membrane to the periplasmic space (*44*). Several discrete regions of SecA are exposed to the periplasm, indicating that large portions of its structure must be altered for it to span the entire inner membrane more than once (*45*−*47*). Additionally, several studies have shown that SecA has two folding domains (*48, 49*). These two folding domains correspond well with the protease-resistant 30 and 65 kDa domains that are thought to be in the membrane (*40, 42*). The extent of interaction between the two domains is influenced by the presence of ADP or ATP (*48, 50*). Because SecA undergoes such pronounced conformational changes during preprotein translocation, determining how it folds in vitro may aid in elucidating how SecA performs its role in vivo.

Here, we report the results of both equilibrium and kinetic studies of the urea-induced unfolding and refolding of SecA. Since SecA is a dimer both in vivo and in vitro (*22*), we use several protein concentrations to determine concentration dependence throughout our equilibrium and kinetic analyses. SecA has been reported to have a stable equilibrium intermediate in its folding pathway (*51*). Our studies indicate that this intermediate is dimeric.

MATERIALS AND METHODS

Chemicals. Ultrapure urea was purchased from ICN. TCEP-HCl[1] and HBVS were from Pierce. TNP-ATP was from Molecular Probes. All other chemicals were reagent grade purchased from common sources.

Buffers. Unless otherwise noted, the buffer used in all studies was 25 mM KAc, 10 mM Hepes, 0.5 mM EDTA, and 100 μM TCEP-HCl, pH 7.6.

SecA Production and Purification. Using a method modified from Mitchell and Oliver (*26*), individual colonies of *E. coli* strain BL21.14 (*secA13(Am) supF(Ts) trp(Am) zch::Tn10 recA::*CAT) containing the plasmid pT7secA2 (*26*) were initially tested for SecA overproduction. The plasmid contains the *secA* gene under T7ϕ10 promoter control. Several individual colonies were grown overnight at 37 °C in 5 mL of Luria broth in the presence of 80 μg/mL ampicillin and 0.2% glucose. The cultures which overproduced SecA were pooled, and a culture was grown overnight in Lin A medium (*52*) in the presence of 80 μg/mL ampicillin and 0.2% glucose at 37 °C. Fresh Lin A medium was inoculated with a 1:50 dilution of the overnight culture in the presence of 0.2% glucose and no ampicillin and grown to a density of 4×10^8 cells/mL at 37 °C. Expression of SecA from the plasmid was induced with 0.1 mM IPTG, and the cells were allowed to grow for another 2 h. The cells were collected by sedimentation at 10 000 rpm in a GSA rotor for 10 min and resuspended in 2 mL of resuspension buffer [25 mM Tris, pH 7.6, 10 mM NaCl, 10 mM Mg(OAc)$_2$, 1 mM DTT] per gram wet weight of cells. The cells were lysed in a French pressure cell at a minimum of 10 000 psi. A protease inhibitor cocktail was immediately added to the lysate (2 μg/mL each of pepstatin, leupeptin, and aprotinin, and 0.5 mM PMSF). All of the following steps were performed at 4 °C. Any remaining intact cells were removed by centrifugation at 12 000 rpm for 20 min in a Sorvall SL50-T rotor. Membranes were removed from the supernatant by sedimentation at 38 000 rpm for 3 h in a Beckman ultracentrifuge using a 60Ti rotor. The supernatant from the high-speed spin was applied to a Blue Sepharose CL-6B column (Pharmacia Biotech) equilibrated with low-salt buffer (LSB: 25 mM Tris, pH 7.6, 10 mM NaCl, 0.5 mM EDTA, 0.5 mM PMSF, and 1 mM DTT) at a flow rate of 2 mL/min. The ∼125 mL column was rinsed with 3 bed volumes of LSB, and then a linear gradient of LSB mixed with high-salt buffer (HSB: 25 mM Tris, pH 7.6, 1.3 M NaCl, 0.5 mM EDTA, 0.5 mM PMSF, 1 mM DTT) was applied to the column. Three to five bed volumes were used to elute SecA from the column. To ensure the complete elution of SecA, the column was rinsed with 4 bed volumes of HSB. Fractions were collected and samples run on a 7.5% SDS−polyacrylamide gel to determine which fractions contained SecA. Fractions containing SecA were pooled, and SecA was precipitated with 50% ammonium sulfate. The precipitated SecA was resuspended in column buffer (25 mM Tris, pH 7.6, 25 mM NaCl, 0.5 mM EDTA, 100 μM DTT) and applied to a Sephacryl S-300 HR column (Pharmacia Biotech) at a flow rate of 0.5 mL/min. The fractions containing SecA were determined as above, and SecA was precipitated with 80% ammonium sulfate. The pellets were

[1] Abbreviations: KAc, potassium acetate; TCEP-HCl, tris(2-carboxyethyl)phosphine hydrochloride; EDTA, ethylenediaminetetraacetic acid; Mg(OAc)$_2$, magnesium acetate; DTT, dithiothreitol; PMSF, phenylmethylsulfonyl fluoride; IPTG, isopropyl β-D-thiogalactopyranoside; HBVS, 1,6-hexane-bis-vinyl sulfone; TNP-ATP, 2′(or 3′)-*O*-(trinitrophenyl)adenosine 5′-triphosphate, trisodium salt.

stored at −80 °C. Before use, the pellets were resuspended in the working buffer (10 mM Hepes, pH 7.6, 25 mM KAc, 0.5 mM EDTA, 100 μM TCEP-HCl) and dialyzed against the working buffer to remove excess ammonium sulfate using a microdialyzer (Gibco-BRL). The SecA was stored in aliquots at −80 °C and was only frozen once; protein was discarded if not used immediately after thawing. The overall yield was ∼12 mg of SecA per liter of cells.

Circular Dichroism and Fluorescence Spectra. Far-UV circular dichroism spectra were collected on a Jasco J-715 spectropolarimeter at 20 °C. The spectra were recorded over the range of 195−300 nm with the SecA concentration at 2.5 μM monomer in 0 and 8 M urea. The step resolution was 0.5 nm with a speed of 50 nm/min. Five scans were accumulated at a bandwidth of 2 nm and a cell path length of 2 mm. Tryptophan fluorescence emission spectra were obtained on an SLM Aminco-Bowman Series 2 Luminescence Spectrometer at 20 °C and were recorded over the range of 305−400 nm with an excitation wavelength of 297 nm using SecA at a concentration of 2.5 μM monomer in both 0 and 8 M urea. The band-passes were set at 4 nm, and the cell path length was 1 cm. The step resolution was 1 nm with a speed of 1 nm/s for all scans.

Unfolding and Refolding of SecA to Equilibrium. SecA in the native state or SecA that had been unfolded in 8 M urea was diluted ∼20-fold into 0−8 M urea and incubated at 20 °C overnight. The final SecA concentrations were 25, 100, or 250 μg/mL, which corresponded to 0.25, 1, and 2.5 μM monomeric SecA, respectively. The unfolding and refolding transitions of SecA were monitored by measuring circular dichroism (CD) and tryptophan fluorescence. CD intensities were determined at 222 nm with a 2 mm path length cuvette and bandwidth of 2 nm. For tryptophan fluorescence, the excitation wavelength was 297 nm, the emission wavelength was 340 nm, and the band-passes were both set to 4 nm with a cell path length of 1 cm. The temperature for all experiments was 20 °C.

HBVS Cross-Linking of SecA in the Presence of Urea. Equilibrium samples from the denatured or native state were prepared as described above with SecA at a concentration of 2.5 μM monomer. The samples were incubated for 3 h. The cross-linker HBVS was added to a final concentration of 140 μM. The reaction was done at 20 °C for 30 min. To stop the reaction, approximately a 10-fold excess of cysteine was added. The products of the cross-linking reaction were run on a 7.5% SDS−polyacrylamide gel.

TNP-ATP Binding Assay. SecA at 1 μM monomer was prepared as described above for the equilibrium experiments. After the protein had reached equilibrium overnight at 20 °C, 1 μM of a nonhydrolyzable ATP analogue (TNP-ATP) was added to each sample. The samples were mixed and read immediately after the addition of the analogue. Excitation and emission wavelengths were set at 410 and 541 nm, respectively, with corresponding band-passes set to 4 and 8 nm.

Kinetic Unfolding and Refolding Experiments. Either native SecA or SecA that had been unfolded in 6.75 M urea was placed in the bottom of a 3 mL cuvette with a 1 cm path length and rapidly diluted to final concentrations of 0.25, 0.6, or 1 μM monomer with buffer containing urea. The unfolding reactions were initiated by at least a 200-fold dilution of native SecA into buffer with urea concentrations ranging from 2 to 3.5 M urea. Refolding reactions were initiated by at least a 90-fold dilution from 6.75 M urea to final concentrations of 0.02−2.5 M urea. These mixtures were not stirred during the course of the experiment to prevent aggregation. All experiments were performed at 20 °C. The manual mixing took approximately 5 s; therefore, the first 5−7 s of recorded data was eliminated to account for instrument response. Excitation and emission wavelengths were 297 and 340 nm, respectively, with the corresponding band-passes at 0.5 and 16 nm. The refractive index was used to determine the final concentrations of urea.

Data Analysis. Equilibrium data were fit to the model: $N_2 \leftrightarrow I_2 \leftrightarrow 2U$, with N_2, I_2, and 2U representing the native dimer, the dimeric intermediate, and the unfolded monomer, respectively, using the program SAVUKA version 5.2, a nonlinear least-squares program (*53*, *54*). Initially, the data for each technique at all concentrations were simultaneously fit using eq 1: where U is the [unfolded protein], T is the

$$[2U^2/(X2*X1)] + (2U^2/X2) + U - T = 0 \qquad (1)$$

[total dimer], $X1$ is equal to $\exp\{-[\Delta G1 - (m1*[\text{urea}])]/RT\}$, and $X2$ is equal to $\exp\{-[\Delta G2 - (m2*[\text{urea}])]/RT\}$. $\Delta G1$ is the ΔG of unfolding from N_2 to I_2 at 1 M standard state conditions, while $\Delta G2$ is the ΔG of unfolding from I_2 to 2U at 1 M standard state conditions, and $m1$ and $m2$ are the m values of the respective transitions. The baseline slopes were fit using eq 2:

$$\begin{aligned} SN &= Sn_o + sn*[\text{urea}] \\ SU &= Su_o + su*[\text{urea}] \\ Z &= (SI - SN)/(SU - SN) \end{aligned} \qquad (2)$$

where SN and SU are the signals of the native and unfolded protein, respectively, at a specific urea concentration and Sn_o and Su_o are the signals in the absence of denaturant, while $sn*$ and $su*$ are the slopes of the native and unfolded baselines, respectively (*55*). The Z-parameter indicates how closely the intermediate resembles the native or unfolded state, with SI the signal of the intermediate. The fitting routine of the Savuka program numerically solved the equations using a bisection algorithm. Subsequently, both CD and fluorescence data at all concentrations were fit globally, also using eqs 1 and 2. The kinetic data were fit to a first-order rate with a single exponent with Kaleidagraph (Synergy Software) from which rates of unfolding or refolding could be obtained using the formula of eq 3 (*56*):

$$F_{(t)} = F_f + (F_i - F_f)e^{-t/\tau} \qquad (3)$$

where F_i and F_f are the initial and final fluorescence intensity, respectively, τ is 1/rate constant, t is time, and $F_{(t)}$ is the change in fluorescence intensity with time. The urea dependence of τ was plotted, and that chevron plot of relaxation times for folding and unfolding was fit to eq 4 (*57*):

$$1/\tau_I = k^{H_2O} \exp(m^{\ddagger}[\text{urea}]/RT) \qquad (4)$$

where k^{H_2O} is the rate constant of the folding or unfolding reaction at 0 M urea and $m^{\ddagger}$ describes the sensitivity of the protein to denaturant. Using the relationship in eq 5, the values for $m^{\ddagger}$ for folding and unfolding can be used to

calculate α which is an approximation of how close the transition state is to the native or intermediate states of the protein.

$$\alpha = m^{\ddagger}_{IN}/(m^{\ddagger}_{IN} - m^{\ddagger}_{NI}) \quad (5)$$

The value of α will be between 0 and 1 with 1 being the nativelike form.

Analytical Ultracentrifugation Equilibrium Sedimentation. SecA that had been unfolded in 8 M urea and subsequently refolded or native SecA was dialyzed against the KAc−Hepes buffer using a microdialyzer from Gibco BRL. The solvent channels of the six-chamber 12 mm external loading analytical ultracentrifuge cells with sapphire windows were loaded with the buffer with which the protein was dialyzed. The corresponding solution channels were loaded with eight concentrations of both native and refolded SecA ranging from 1 to 15 μM monomer (0.1−1.5 mg/mL). The samples were centrifuged in a Beckman XLI ultracentrifuge at 12 000 and 15 000 rpm at 20 °C in an AN60Ti 8 hole rotor until sedimentation equilibrium was achieved at each speed. Interference optics were used to follow the concentration gradient as well as monitor the approach of the solution to equilibrium in the cells every 3 h. Attainment of equilibrium was verified using the MATCH program (personal communication, D. Yphantis). Prior to the experimental run, the cells were aged and water blanks were obtained (*58*). After the data were collected from the experimental run, the cells were cleaned and loaded with water, and another set of water blank scans were taken at the two speeds. After comparison with the initial water blank to ensure that no major change had occurred, the final water blank was subtracted from the data to correct for systematic noise due to cell distortion. The final equilibrium data were fit to specific models using a nonlinear least-squares program, NONLIN (*59*). Using the program SEDNTERP (*60*), the dimer molecular weight (MW = 203 800) and the partial specific volume ($\bar{v}$ = 0.7334) were determined from the amino acid composition (*61*), and the density of the buffer (ρ = 0.99976) was determined using the value of buffer constituents.

Analytical Ultracentrifugation Velocity Sedimentation. Double-sector 12 mm analytical ultracentrifuge cells with sapphire windows were loaded with both buffer and native SecA at 1.58 or 0.158 mg/mL, or refolded SecA at 1.78 or 0.178 mg/mL. The samples were centrifuged in a Beckman XLI ultracentrifuge at 50 000 rpm at 20 °C in an AN60Ti rotor until SecA was sedimented to the bottom of the cell. The progress of the sedimentation of the protein was monitored by scanning the cell radially once per minute in 10 μm increments using interference optics. The data were analyzed using the program DCDT (*62*). From this program, the weight average sedimentation coefficient (s_w) was determined. Using the two protein concentrations, the sedimentation constant ($s^{\circ}_{20,w}$) for each protein was determined by extrapolating the values of s_w to zero concentration. In addition, the program Svedberg (*63*) was used to directly fit the data and determine the sedimentation and diffusion coefficients (*s* and *D*) which were used to estimate the molecular weight from the *s*:*D* ratio. If several species are present, the observed *D* obtained from the resulting wider boundary would be larger than expected. This result would indicate an apparently low molecular weight, thus giving a measure of the impurity of the sample. The program SEDNTERP (*60*) was used to model the hydrodynamic properties of the SecA dimer from the value of $s^{\circ}_{20,w}$.

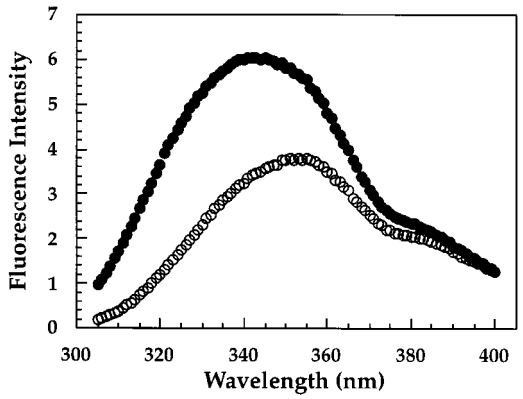

FIGURE 1: Fluorescence emission spectra of native SecA (●) and SecA unfolded in 8 M urea (○). The excitation wavelength was 280 nm. The protein concentration was 2.5 μM monomer (250 μg/mL).

RESULTS

We have chosen to investigate the folding of SecA as a model for the folding of large, multimeric proteins. SecA was a likely candidate for these experiments because several investigators have refolded SecA for a variety of experiments (*48, 49, 51*). Additionally, large quantities of the protein are reasonably easy to purify. In addition, SecA possesses an interesting in vivo role which involves several conformations that can be induced by the binding of ligands (*48, 50*). For these reasons, we find SecA an intriguing protein for folding studies.

In order for SecA to serve as a useful model for the folding of large proteins, the SecA folding pathway must first be characterized. The order in which the subunits and domains interact as well as the stability of these interactions needs to be determined. Also, the rate-limiting step in folding must be resolved. Several experimental approaches were used to elucidate the pathway.

The Unfolding of SecA Can Be Monitored by Tryptophan Fluorescence and Circular Dichroism. To determine if a difference in native and denatured SecA could be detected using tryptophan fluorescence and circular dichroism (CD), the spectra of both native and denatured SecA were measured. Tryptophan fluorescence and CD are convenient spectral probes for observing tertiary and secondary structure, respectively, during folding. After excitation at 280 nm, native SecA had an emission maximum of 342 nm (Figure 1). SecA denatured in 8 M urea had a fluorescence intensity ~65% that of native SecA and an emission maximum that was shifted to 355 nm. This decrease in fluorescence intensity and red shift indicated that one or more of the seven tryptophans of SecA became more solvent-exposed during unfolding (*64*). The far-UV CD spectra for native SecA and SecA in 8 M urea are shown (Figure 2). Native SecA had a CD spectrum typical of an α-helical protein, with double minima at 209 and 222 nm. SecA in 8 M urea had a CD spectrum that showed virtually no secondary structure present, indicating that significant unfolding had occurred.

SecA Folds via a Dimeric Intermediate. To determine the ΔG of stabilization for the SecA dimer, either native or

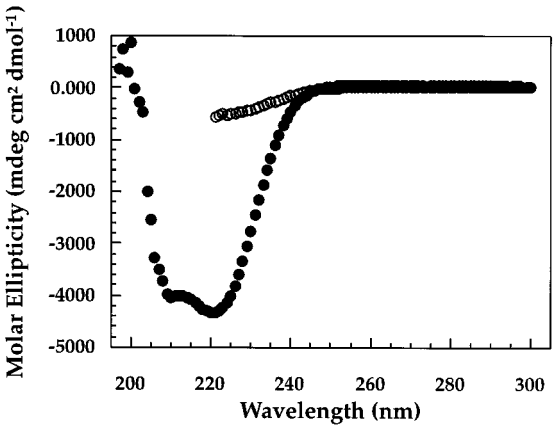

FIGURE 2: CD spectra of native SecA (●) and SecA unfolded in 8 M urea (○). The protein concentration was 2.5 μM monomer (250 μg/mL).

denatured SecA was incubated in various concentrations of urea until equilibrium was reached. Both tryptophan fluorescence and circular dichroism (CD) at 222 nm were used to monitor the fraction of unfolded SecA. The reactions were reversible, although the transitions from the two techniques did not give coincident curves (Figure 3). A plateau was observable by both methods between 2.5 and 5 M urea. Protein concentration dependence was only apparent at the urea concentrations of the plateau, suggesting that the plateau corresponded to a dimer to monomer transition. To confirm the presence of a dimeric intermediate, cross-linking experiments were done at urea concentrations where the putative dimeric intermediate was populated (Figure 4). Because of the presence of urea, an amino-specific cross-linking reagent could not be used. Therefore, we chose a cysteine-reactive cross-linker. There are 4 cysteines in SecA at positions 98, 885, 887, and 896 (*65*, *66*). Cross-linked dimers were present in samples of SecA incubated in 2.5, 3.5, and 4 M urea, concentrations where the plateau was observed. There was little cross-linked dimer when SecA was incubated in 8 M urea, which fully denatures it, indicating that the cross-linking was specific. There was also little cross-linking at 0 M urea, which suggested that the cysteines were less accessible without urea present. In the absence of the cross-linker, some disulfide-linked dimers were present, which confirmed the results of our cross-linking experiment. Little higher order cross-linking was observed on the gel which indicated that the intermediate was unlikely to have more than two subunits.

Since the cross-linking experiments were consistent with a dimeric intermediate in the folding pathway of SecA, the data were fit to the model $N_2 \leftrightarrow I_2 \leftrightarrow 2U$ (eq 1) using the program SAVUKA version 5.2 (Table 1). We also tried to fit the data to the two-state model, $N_2 \leftrightarrow 2U$. These fits were poor (data not shown). Using the three-state fit, an overall ΔG of -22.5 ± 2.7 kcal mol^{-1} indicates that SecA is stable. The *m*-values, which signify the change in the amount of solvent exposure from the native to the denatured state (*67*), were 4.1 ± 0.8 and 1.5 ± 0.2 kcal mol^{-1} M^{-1} for the first and second transitions, respectively. These values suggested that the first transition from $N_2 \rightarrow I_2$ exposed a greater amount of protein to the solvent than did the $I_2 \rightarrow 2U$ transition. The *Z*-parameter is an expression of the extent that the optical properties of the intermediate are like the unfolded protein (*54*). The *Z*-parameter of the SecA unfolding

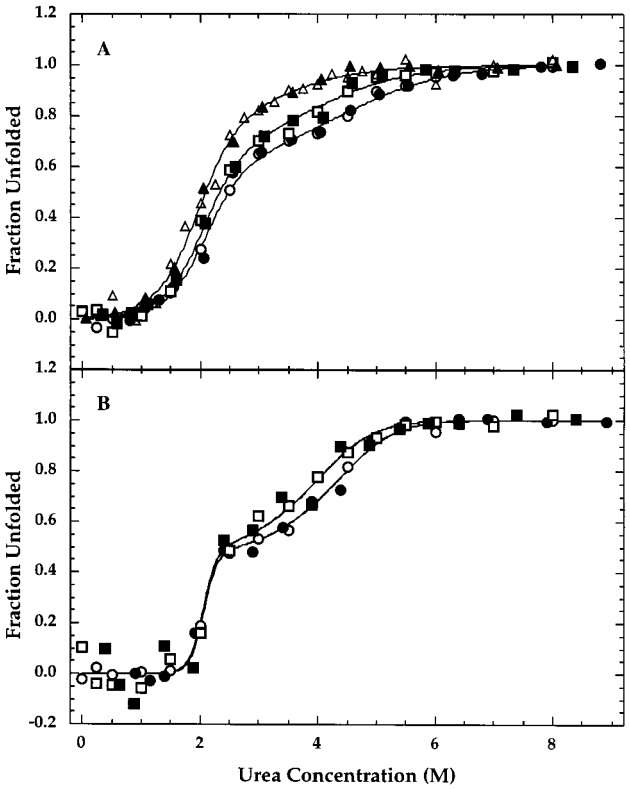

FIGURE 3: Equilibrium unfolding and refolding of SecA. In (A), the transition was monitored by tryptophan fluorescence. The excitation wavelength was 297 nm, and the emission wavelength was 340 nm. In (B), the transition was monitored using circular dichroism. The measurements were taken at 222 nm with a 2 mm path length cuvette and a band-pass of 2 nm. Unfolding (open symbols) and refolding (closed symbols) reactions are at the following concentrations of monomer: 2.5 μM (●,○), 1.0 μM (■,□), and 0.25 μM (▲,△). The lines shown are the simultaneous fit of the data for each technique at all protein concentrations to the model: $N_2 \leftrightarrow I_2 \leftrightarrow 2U$ using the program SAVUKA. The CD and fluorescence data at all concentrations were also globally fit to the same model, the results of which are shown in Table 1.

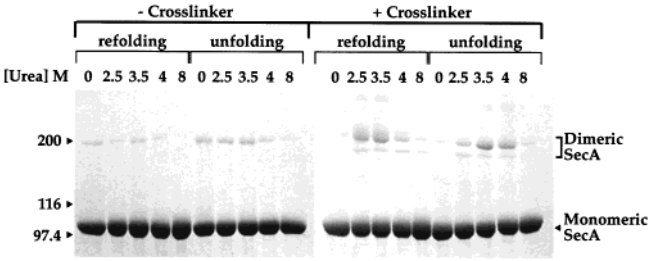

FIGURE 4: Cross-linking of SecA by HBVS. Either native or unfolded SecA (2.5 μM monomer) was equilibrated in different concentrations of urea at 20 °C. SecA was further incubated for 30 min in the presence or absence of cross-linker (140 μM). The protein was run on a 7.5% SDS−polyacrylamide gel. Monomeric SecA ran at ~102 kDa while dimeric SecA ran at ~200 kDa. The molecular mass markers are in kilodaltons.

transition was ~0.5, which means that the intermediate in the folding pathway of SecA contained approximately equal amounts of nativelike and unfolded optical properties. The larger error in the ΔG and *m*-values for the first transition was likely due to the steep slope of the curve (high *m*-value). We also investigated the stability of SecA in buffer with 300 mM KAc, using equilibrium unfolding, to determine if salt altered the folding of SecA. No difference in stability was seen (data not shown).

Table 1: Thermodynamic Parameters As Determined from Equilibrium Experiments[a]

technique	$\Delta G^\circ_{N2/I2}$ (kcal/mol)	$-m_{N2/I2}$ (kcal mol^{-1} M^{-1})	$\Delta G^\circ_{I2/2U}$ (kcal/mol)	$-m_{I2/2U}$ (kcal mol^{-1} M^{-1})	*Z*-parameter
fluorescence[b]	4.2 ± 0.7	1.9 ± 0.3	10.7 ± 0.9	0.78 ± 0.20	0.50 ± 0.15
CD	10.9 ± 5.0	5.3 ± 2.5	14.1 ± 1.6	1.5 ± 0.4	0.45 ± 0.09
global fit[c]	8.4 ± 1.6	4.1 ± 0.8	14.1 ± 1.1	1.5 ± 0.2	0.49 ± 0.06

[a] Data were fit to the apparent three-state model: $N_2 \leftrightarrow I_2 \leftrightarrow 2U$. [b] Fluorescence and CD fits were performed concurrently at the following concentrations: fluorescence at 0.25, 1, and 2.5 μM monomer and CD at 1 and 2.5 μM monomer. [c] The above fluorescence and CD data were fit simultaneously for the global fit.

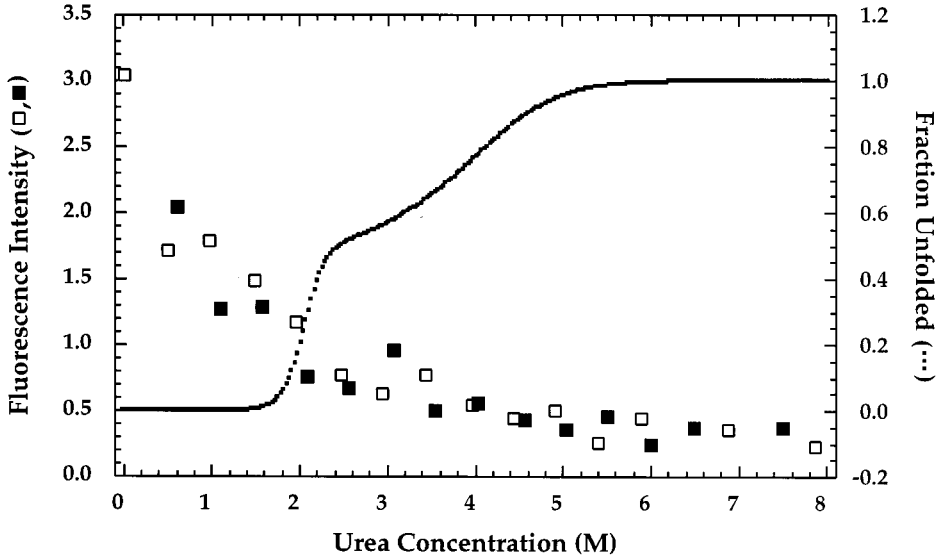

FIGURE 5: Dependence of binding of a nonhydrolyzable fluorescent ATP analogue (TNP-ATP) on the urea concentration. The protein concentration for both the unfolding (□) and refolding (■) reactions was 1 μM monomer. The concentration of TNP-ATP was also 1 μM. The dotted line (· · ·) was the model fit from the equilibrium folding experiments monitored by CD at 1 μM monomer taken from Figure 3B.

The N-Terminal Domain Unfolds Prior to Subunit Dissociation. To determine at what urea concentration the high-affinity ATP binding site in the N-terminal domain loses the ability to bind ATP, equilibrium unfolding and refolding reactions were monitored using a fluorescent nonhydrolyzable ATP analogue, TNP-ATP. This analogue is fluorescent when bound in a hydrophobic binding pocket and has little fluorescence when exposed to solvent. Therefore, it provides a useful probe for disruption of the binding domain (*68*, *69*). The concentration of TNP-ATP was held at 1 μM so that only the high-affinity ATP binding site in the amino-terminal domain would be occupied by the analogue. The dependence of TNP-ATP binding on the urea concentration is shown in Figure 5. The loss of fluorescence began immediately upon the addition of urea and continued until ~3.5 M urea, with the majority of fluorescence lost prior to 2.5 M urea. The decrease in fluorescence correlated well with the formation of the intermediate observed in the equilibrium curves monitored by CD and tryptophan fluorescence, since ~85% of the fluorescence was lost by 2.2 M urea where the dimeric intermediate is stably populated. Thus, the N domain unfolds at lower urea concentrations than required for dissociation of the subunits.

Domain Association Is the Rate-Limiting Step in the Folding of SecA. From the previous equilibrium experiments, we determined that dimeric SecA was a stable protein. This stability should be accompanied by a relatively fast rate of folding and slow rate of unfolding (*70*). Kinetic unfolding and refolding reactions were done to further investigate the folding of SecA. The intrinsic fluorescence of tryptophans was used to follow the kinetic reactions. When native SecA was rapidly diluted with various concentrations of buffered urea, there was a decrease in fluorescence due to unfolding which reached equilibrium with time (Figure 6A). The unfolding kinetics fit well to a first-order single-exponential equation (eq 3), as shown by the residuals of the fit to the data (Figure 6A). These data were also fit with a first-order equation with two exponents which provided no increase in the accuracy of the fit. The unfolding kinetics appeared to have a small burst phase of about 10% of the total observable fluorescence change (data not shown). Thus, there may be a fast kinetic phase which cannot be resolved by this method. To initiate refolding, unfolded SecA was diluted with buffer or buffer with various concentrations of urea. An increase in fluorescence over time was observed (Figure 6B). The refolding kinetics had a large burst phase of 50% of the total observable fluorescence change (data not shown). As with the kinetic unfolding reactions, the refolding reactions appear to be monophasic and were well fit using a first-order single-exponential equation. Again, when the data were fit to a first-order equation with two exponents, there was no decrease in the error of the fit nor was there any improvement in the residuals, thus indicating that additional parameters were unnecessary (*71*). Since SecA is a dimer, it might be expected that refolding would require a second-order equation. These reactions were tested to determine if they were second order by plotting the rate constant versus protein concentration. No protein concentration dependence in the rate constants

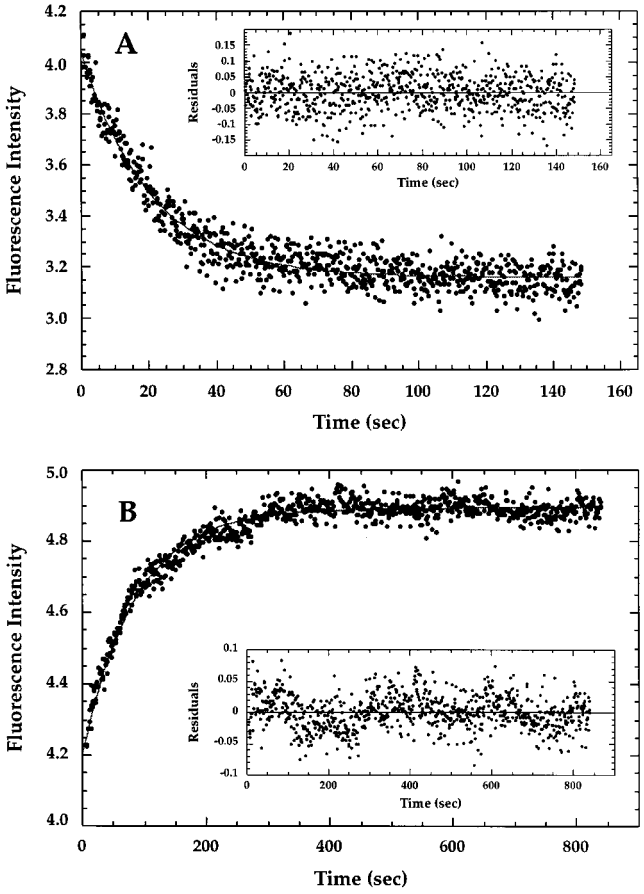

FIGURE 6: Kinetics of unfolding (A) and kinetics of refolding (B) of SecA. Native or unfolded SecA was rapidly diluted by adding buffer with various concentrations of urea. The final protein concentrations were 25, 60, and 100 μg/mL (0.25, 0.6, and 1 μM monomer). Shown here are representative kinetic experiments at 60 μg/mL (A) and 100 μg/mL (B). The excitation wavelength was 297 nm, and the emission wavelength was 340 nm. The interior panel shows the residuals between the experimental points and the theoretical curve.

was observed, indicating the reactions were not second order (data not shown). It is possible that dimer association occurs so rapidly that it cannot be resolved using manual mixing techniques. The scatter in the refolding curve, and residuals, was presumably due to some aggregation. Because SecA only regains ~80% of its intrinsic fluorescence during folding, a loss of protein, most likely due to aggregation, was indicated. Although the scatter was present in every refolding reaction, it was not systematic between reactions. Even repeated experiments at the same urea and protein concentrations gave different residuals. Consequently, we believe it unlikely that additional exponents are necessary for fitting these data.

The apparent rate constants were dependent on the urea concentration (Figure 7). The data were fit using eq 4. The values for the relaxation time of the folding and unfolding reactions in the absence of urea, as well as the values for $m^{\ddagger}$, are consistent with SecA being a stable dimer (Table 2). The error in the $\tau_u^{H_2O}$ is likely due to the large $m^{\ddagger}$ and long extrapolation to 0 M urea. No protein concentration dependence was observed for either the unfolding or the refolding reactions. This result was expected since the peak of the chevron plot occurs at a urea concentration which is similar to the midpoint of the $N_2 \leftrightarrow I_2$ transition in the fluorescence equilibrium curve. This is also consistent with the observation

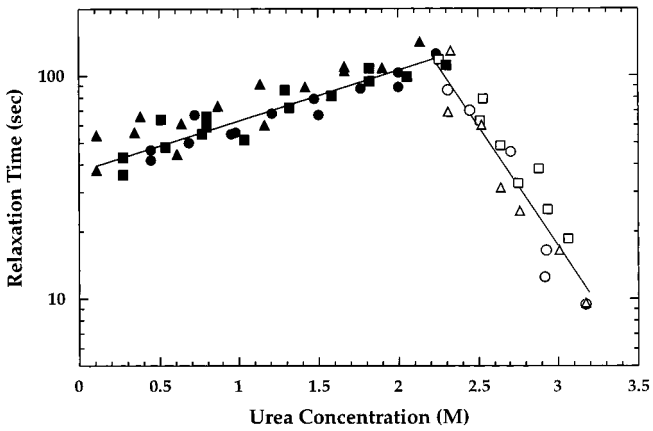

FIGURE 7: Dependence of the unfolding (open symbols) and refolding (closed symbols) relaxation times for SecA at concentrations of 1 μM (●,○), 0.6 μM (■,□), and 0.25 μM (▲,△) monomer. Both unfolding and refolding kinetics were monitored using intrinsic tryptophan fluorescence. The lines show a fit of the relaxation times for both unfolding and refolding to eq 2.

Table 2: Kinetic Parameters for Unfolding and Refolding[a]

	τ^{H_2O} (s)	$m^{\ddagger}$ (kcal mol^{-1} M^{-1})
$N_2 \rightarrow I_2$	33300 ± 26600	−1.48 ± 0.19
$I_2 \rightarrow N_2$	37.90 ± 2.64	0.31 ± 0.02

[a] Fits of the urea dependence on τ were performed concurrently with protein at the following concentrations: 0.25, 0.6, and 1 μM monomer.

that the kinetics were not second order and did not require two rates to be fit well. No urea-independent phase was apparent, indicating that cis−trans proline isomerization did not occur during folding of SecA. The value of α (eq 5) for the transition state of SecA was 0.172, indicating that the transition state between N_2 and I_2 was more like the intermediate than the native state with the exposure of large portions of hydrophobic surface (*72*). These data suggested that the rate-limiting step in the folding of SecA was from the dimeric intermediate to the native dimer.

SecA Refolds into a Dimer. To analyze the data as we have, it was necessary to confirm that SecA refolded into a dimer. Therefore, we used equilibrium and velocity sedimentation on both native and refolded SecA. The equilibrium sedimentation data for SecA were fit with both the ideal and nonideal single species models. In addition, the data were fit to the following models: monomer−dimer, monomer−trimer, monomer−tetramer, monomer−dimer−trimer, and monomer−dimer−tetramer. From the ideal fit, the *Z*-average molecular mass (M_z) was determined (personal communication, D. Yphantis). For native SecA, an M_z of approximately 191 kDa was obtained, consistent with a dimer. An rms value of 1.36×10^{-2} fringes (compared with blank values of 1×10^{-2} fringes) and little systematic error indicated a good fit to this model (data not shown). Other fits were not significantly different, and all fits indicated the dimer was the basic structure present. By fitting the equilibrium data with the various self-association models as indicated above, we determined that little or no association of SecA occurred beyond the dimer. Since no monomer was detectable once SecA reached equilibrium, the SecA dimer, in the absence of denaturant, was stable with any monomer concentration being below that detectable by the optics of the instrument. This indicates that the K_d was less than 0.6 μM. The values

for refolded SecA were similar to those described for the native SecA.

From velocity sedimentation, the sedimentation constants $s_{20,w}$ for both native and refolded SecA were determined to be 8.65 ± 0.08 and 9.39 ± 0.08 S, respectively, using the program DCDT (*62*). When the raw data were fit using the program Svedberg (*63*), $s_{20,w}$ values of 8.439 ± 0.003 and 8.681 ± 0.009 S for both the native and the refolded SecA respectively, were determined. In addition, the averaged MW was estimated to be 180 000. This approximate MW, determined from the *s*:*D* ratio, was in fair agreement with that calculated from the amino acid composition for the SecA dimer (204 000) and indicated that the sample was reasonably homogeneous. The SecA dimer was modeled by SEDNTERP using the determined value of $s_{20,w}$, both the sequence-based (molecular) and the calculated values of MW, and the values of $\bar{v}$ and hydration. The model that best fit the data was a prolate ellipsoid shaped molecule with an axial ratio of 4.3:1. Our value compares with the value of 2:1 axial ratio determined by small-angle X-ray scattering (*73*).

DISCUSSION

The study of protein folding has been primarily limited to small, single-domain proteins with two-state transitions. Since many proteins in the cell have multiple subunits as well as multiple domains, those studies are not sufficient to explain the folding of all proteins. We have chosen to use the protein SecA as a model for the folding of large, multidomain, multimeric proteins because it is a dimer with a monomer molecular weight of 102 000 (*22*). Additionally, SecA has been shown to have at least two major functional domains as well as several subdomains (*48, 49*).

The in Vitro Folding of SecA Is through a Three-State Pathway. In previous studies, SecA was shown to reversibly unfold and refold (*33, 51*). Here, we conclude that the folding pathway of SecA contains a stable dimeric intermediate. This conclusion was reached because there is a significant plateau in the equilibrium folding experiments and concentration dependence was only observed in the plateau region of the curves. Also, cross-linking studies indicated that SecA remained dimeric at urea concentrations where the intermediate was populated. Therefore, we fit the data to a three-state model including a dimeric intermediate, $N_2 \leftrightarrow I_2 \leftrightarrow 2U$. SecA was stable, with an overall ΔG of −22.5 kcal/mol. The results of the equilibrium experiment measuring the TNP-ATP fluorescence showed that the loss of fluorescence corresponded with the formation of the dimeric intermediate in the $N_2 \leftrightarrow I_2$ transition. Since the concentration of ATP analogue used for this experiment was low enough to saturate only the high-affinity site located in the N-domain of SecA (*26*), it was the unfolding of the N-terminal domain that resulted in the loss of binding of the TNP-ATP. The *Z*-parameter, obtained from the equilibrium folding studies, indicates that the I_2 intermediate has optical properties of a protein with 50% nativelike and 50% unfolded structure, which is consistent with the proposed unfolding of the amino terminus. The C-terminal portion of SecA contains the putative dimerization region (*35*), and, therefore, our conclusion that the intermediate is a dimer is reasonable. The kinetic data are also consistent with the formation of a dimeric intermediate as an essential step in the folding of functional SecA.

The results of the equilibrium experiments indicated that SecA was a stable protein. As such, SecA should have kinetics which reflect this stability, including a fast rate of folding and a slow rate of unfolding (*70*). The slow $\tau_U^{H_2O}$ of 33 300 ± 26 600 s indicated that SecA was unlikely to unfold from the native state. The $\tau_F^{H_2O}$ of 37.9 ± 2.6 was slow as compared to many small proteins such as monomeric λ repressor, barnase, and streptococcal Protein G (*56, 74, 75*). However, many large multidomain proteins such as bacterial luciferase, malate dehydrogenase, and UDP glucose dehydrogenase (*12, 76*) have much slower refolding kinetics than SecA, suggesting that SecA has fast folding kinetics for a protein of its size.

The Folding of Large Proteins Is More Complex than a Two-State System. The model we have determined for SecA is $N_2 \leftrightarrow I_2 \leftrightarrow 2U$, a three-state model with the native dimer, a dimeric intermediate, and the unfolded monomers. This model is not uncommon for dimeric proteins (*21, 77*), but it may be too simplistic for a protein as large as SecA. The burst phase in folding may indicate another intermediate along the kinetic folding pathway. Alternatively, the burst phase may be the dimerization process occurring. One protein which has a complex folding pathway with similarities to SecA is creatine kinase (*78*). Creatine kinase has a burst phase intermediate, as well as an equilibrium intermediate. A common feature between SecA and creatine kinase appears to be that the slow step in folding is domain association in the $I_2 \rightarrow N_2$ transition. Also, in both proteins, dimer formation occurs quickly during folding.

Aggregation is often a problem for large proteins due to their slower folding and the fact they are too large to use chaperones. The most common type of chaperones in bacterial cells are the chaperonins GroEL/S, which are members of the hsp60 and hsp10 family of heat shock proteins (*79*). The internal cavity of GroEL, where the folding has been shown to take place, is only large enough for a protein of ~60 kDa to enter (*80*). Therefore, a protein such as SecA is too large to use GroEL as a chaperone. Although other studies have suggested that GroEL may bind to SecA in vivo (*81*), in in vitro experiments using sucrose gradients (data not shown), we have been unable to show any interaction between native or unfolded SecA and GroEL. Since SecA rapidly forms a dimeric intermediate which is quite stable, the mechanism of fast dimerization may aid SecA and other multimeric proteins such as creatine kinase (*78*) in avoiding the nonproductive pathway that leads to aggregation.

The stability of SecA appears similar to that of other dimeric proteins, such as *E. coli* Trp repressor, creatine kinase, and bacterial luciferase (*20, 21, 78*). The stability of the average dimeric protein seems to be higher than that of the average monomeric protein, indicating that subunit−subunit interaction can greatly increase the stability of a protein, most likely due to the burial of hydrophobic surfaces (*77*). In the unfolding of SecA, the *m*-value for the $N_2 \rightarrow I_2$ transition was greater than that of the second transition. One might expect that subunit dissociation would cause a greater amount of hydrophobic surface to be exposed to solvent than in domain unfolding, as has been shown for the folding of organophosphorus hydrolase (*77*). Possibly the amount of buried surface area at the subunit interface in SecA is not as great as for organophosphorus hydrolase, and domain

unfolding actually does expose more surface area to the solvent. The fact that there is a 50% loss in both secondary and tertiary structure, as indicated by the *Z*-parameter from the equilibrium experiments, suggested that a large portion of SecA unfolded during the $N_2 \rightarrow I_2$ transition. This could cause a large exposure of surface area to solvent and may explain the seeming discrepancy in the *m*-values. Also, SecA is a large protein, and the dimerization region is small compared to the full-length protein (*35*). Thus, this result might be expected for the folding of SecA.

The Role of SecA in Vivo. From earlier studies, SecA was shown to have two folding domains (*48*−*51*), and each domain appears to have multiple functional roles. The amino-terminal domain contains the high-affinity nucleotide binding site (*26*, *27*) and the putative precursor protein binding site (*82*), and appears to insert through the membrane to the periplasm (*37*, *42*, *45*). The carboxy-terminal domain contains the low-affinity nucleotide binding site (*26*, *27*), the SecB (*34*) and SecY binding sites (*36*, *37*), the anionic phospholipid binding region (*38*), and the putative dimerization region (*35*), and also spans the membrane to expose itself to the periplasm (*37*, *42*, *43*, *45*). SecA has been proposed to undergo some form of unfolding event, most likely into a molten globule-like form, in order to insert itself into the inner membrane (*41*). The mechanism by which SecA undergoes this unfolding event is not clear. Previous studies have indicated that the extreme C-terminus is unstable and unfolds at low guanidine hydrochloride concentrations (*51*). The complete unfolding of the carboxy terminus is unlikely due to the recent finding that the SecB binding site on SecA is stabilized by a Zn^{2+} ion (*39*). Our study indicates that the N-terminal domain unfolds prior to subunit dissociation, suggesting that the interactions that stabilize the N domain are weak when compared to those of the subunit interface. Thus, what may actually occur in vivo is that both domains partially unfold and change conformation, thereby allowing each to insert into the membrane even while SecA remains a dimer.

ACKNOWLEDGMENT

We thank Drs. Arlene Alberts and Philip Yeagle for the use of the Jasco Spectropolarimeter, Dr. James Knox for the use of the Silicon Graphics Octane, and Eric Anderson and Dana Wang for help with the analytical ultracentrifuge and data analysis. We are extremely grateful to Dr. C. Robert Matthews and Dr. Osman Bilsel for their help with the fitting program Savuka and for critical discussions of the manuscript. We also thank Lili Aramli and Carole Capen for their helpful discussions and critical reading of the manuscript.

REFERENCES

1. Anfinsen, C. B. (1973) *Science 181*, 223−230.
2. Welch, W. J., and Brown, C. R. (1996) *Cell Stress Chaperones 1*, 99−108.
3. Thomas, P. J., Qu, B.-H., and Pedersen, P. L. (1995) *Trends Biochem. Sci. 20*, 456−459.
4. Marston, F. A. O. (1986) *Biochem. J. 240*, 1−12.
5. Mitraki, A., and King, J. (1989) *Bio/Technology 7*, 690−697.
6. Betts, S., Haase-Pettengell, C., and King, J. (1997) *Adv. Protein Chem. 50*, 243−264.
7. Jaenicke, R. (1987) *Prog. Biophys. Mol. Biol. 49*, 117−237.
8. Kim, P. S., and Baldwin, R. L. (1982) *Annu. Rev. Biochem. 51*, 459−489.
9. Jennings, P. A., Finn, B. E., Jones, B. E., and Matthews, C. R. (1993) *Biochemistry 32*, 3783−3789.
10. Ptitsyn, O. B. (1992) in *Protein Folding* (Creighton, T., Ed.) pp 243−300, W. H. Freeman and Co., New York.
11. Garel, J.-R. (1992) in *Protein Folding* (Creighton, T., Ed.) pp 405−454, W. H. Freeman and Co., New York.
12. Jaenicke, R., and Rudolph, R. (1989) *Protein structure: a practical approach*, IRL Press, Oxford.
13. Waddle, J. J., Johnston, T. C., and Baldwin, T. O. (1987) *Biochemistry 26*, 4917−4921.
14. Ziegler, M. M., Goldberg, M. E., Chaffottee, A. F., and Baldwin, T. O. (1993) *J. Biol. Chem. 268*, 10760−10765.
15. Goldenberg, D., and King, J. (1981) *J. Mol. Biol. 145*, 633−651.
16. Haase-Pettingell, C. A., and King, J. (1997) *J. Mol. Biol. 267*, 88−102.
17. Garel, J. R., and Dautry-Varsat, A. (1980) *Proc. Natl. Acad. Sci. U.S.A. 77*, 3379−3383.
18. Beasty, A. M., Hurle, M. R., Manz, J. T., Stackhouse, T., Onuffer, J. J., and Matthews, C. R. (1986) *Biochemistry 25*, 2965−2974.
19. Gittelman, M. S., and Matthews, C. R. (1990) *Biochemistry 29*, 7011−7020.
20. Clark, A. C., Sinclair, J. F., and Baldwin, T. O. (1993) *J. Biol. Chem. 268*, 10773−10779.
21. Gloss, L. M., and Matthews, C. R. (1997) *Biochemistry 36*, 5612−5623.
22. Akita, M., Shinkai, A., Matsuyama, S., and Mizushima, S. (1991) *Biochem. Biophys. Res. Commun. 174*, 211−216.
23. Cabelli, R. J., Dolan, K. M., Qian, L., and Oliver, D. B. (1991) *J. Biol. Chem. 266*, 24420−24427.
24. Lill, R., Cunningham, K., Brundage, L. A., Ito, K., Oliver, D., and Wickner, W. (1989) *EMBO J. 8*, 961−966.
25. Matsuyama, S., Kimura, E., and Mizushima, S. (1990) *J. Biol. Chem. 265*, 8760−8765.
26. Mitchell, C., and Oliver., D. (1993) *Mol. Microbiol. 10*, 483−497.
27. den Blaauwen, T., and Driessen, A. J. (1996) *Arch. Microbiol. 165*, 1−8.
28. Hartl, F.-U., Lecker, S., Schiebel, E., Hendrick, J. P., and Wickner, W. (1990) *Cell 63*, 269−279.
29. Fandl, J. P., Cabelli, R., Oliver, D., and Tai, P. C. (1988) *Proc. Natl. Acad. Sci. U.S.A. 85*, 8953−8957.
30. Matsumoto, G., Yoshihisa, T., and Ito, K. (1997) *EMBO J. 16*, 6384−6393.
31. Lill, R., Dowhan, W., and Wickner, W. (1990) *Cell 60*, 271−280.
32. Hendrick, J. P., and Wickner, W. (1991) *J. Biol. Chem. 266*, 24596−24600.
33. Driessen, A. J. M. (1993) *Biochemistry 32*, 13190−13197.
34. Fekkes, P., van der Does, C., and Driessen, A. J. M. (1997) *EMBO J. 16*, 6105−6113.
35. Hirano, M., Matsuyama, S., and Tokuda, H. (1996) *Biochem. Biophys. Res. Commun. 229*, 90−95.
36. Snyders, S., Ramamurthy, V., and Oliver, D. (1997) *J. Biol. Chem. 272*, 11302−11306.
37. Ramamurthy, V., and Oliver, D. (1997) *J. Biol. Chem. 272*, 23239−23246.
38. Breukink, E., Nouwen, N., van Raalte, A., Mizushima, S., Tommassen, J., and de Kruijff, B. (1995) *J. Biol. Chem. 270*, 7902−7907.
39. Fekkes, P., de Wit, J. G., Boorsma, A., Friesen, R. H. E., and Driessen, A. J. M. (1999) *Biochemistry 38*, 5111−5116.
40. Eichler, J., and Wickner, W. (1997) *Proc. Natl. Acad. Sci. U.S.A. 94*, 5574−5581.
41. Ulbrandt, N. D., London, E., and Oliver, D. B. (1992) *J. Biol. Chem. 267*, 15184−15192.
42. Economou, A., and Wickner, W. (1994) *Cell 78*, 835−843.
43. Oliver, D. B. (1993) *Mol. Microbiol. 7*, 159−165.
44. Schiebel, E., Driessen, A. J. M., Hartl, F.-U., and Wickner, W. (1991) *Cell 64*, 927−939.
45. Kim, Y. J., Rajapandi, T., and Oliver, D. (1994) *Cell 78*, 845−853.

46. van der Does, C., den Blaauwen, T., de Wit, J. G., Manting, E. H., Groot, N. A., Fekkes, P., and Driessen, A. J. M. (1996) *Mol. Microbiol. 22*, 619−629.
47. Eichler, J., and Wickner, W. (1998) *J. Bacteriol. 180*, 5776−5779.
48. den Blaauwen, T., Fekkes, P., de Wit, J. G., Kuiper, W., and Driessen, A. J. M. (1996) *Biochemistry 35*, 11994−12004.
49. Karamanou, S., Vrontou, E., Sianidis, G., Baud, C., Roos, T., Kuhn, A., Politou, A. S., and Economou, A. (1999) *Mol. Microbiol. 34*, 1133−1145.
50. Price, A., Economou, A., Duong, F., and Wickner, W. (1996) *J. Biol. Chem. 271*, 31580−31584.
51. Song, M., and Kim, H. (1997) *J. Biochem. 122*, 1010−1018.
52. Rhoads, D. B., Tai, P. C., and Davis, B. (1984) *J. Bacteriol. 159*, 63−70.
53. Zitzewitz, J. A., Bilsel, O., Luo, J., Jones, B. E., and Matthews, C. R. (1995) *Biochemistry 34*, 12812−12819.
54. Bilsel, O., Zitzewitz, J. A., Bowers, K. E., and Matthews, C. R. (1999) *Biochemistry 38*, 1018−1029.
55. Gualfetti, P. J., Bilsel, O., and Matthews, C. R. (1999) *Protein Sci. 8*, 1623−1635.
56. Ghaemmaghami, S., Word, J. M., Burton, R. E., Richardson, J. S., and Oas, T. G. (1998) *Biochemistry 37*, 9179−9185.
57. Gloss, L. M., and Matthews, C. R. (1998) *Biochemistry 37*, 15990−15999.
58. Ansevin, A. T., Roark, D. E., and Yphantis, D. A. (1970) *Anal. Biochem. 34*, 237−261.
59. Johnson, M., Correia, J. J., Yphantis, D. A., and Halvorson, H. R. (1981) *Biophys. J. 36*, 575−588.
60. Laue, T. M., Shah, B. D., Ridgeway, T. M., and Pelletier, S. L. (1992) in *Analytical Ultracentrifugation in Biochemistry and Polymer Science* (Harding, S. E., Rowe, A. J., and Horton, J. G., Eds.) pp 90−125, The Royal Society of Chemistry, Cambridge.
61. Cohn, E., and Edsall, J. (1943) *Proteins, amino acids and peptides as ions and dipolar ions*, Vol. XVIII, Reinhold Publishing Corp., New York.
62. Stafford, W. F. (1992) in *Analytical Ultracenrifugation in Biochemistry and Polymer Science* (Harding, S. E., Rowe, A. J., and Horton, J. G., Eds.) pp 359−393, The Royal Society of Chemistry, Cambridge.
63. Philo, J. S. (1997) *Biophys. J. 72*, 435−444.
64. Lakowicz, J. R. (1983) *Principles of Fluorescence Spectroscopy*, Plenum Press, New York.
65. Schmidt, M. G., Rollo, E. E., Grodberg, J., and Oliver, D. B. (1988) *J. Bacteriol. 170*, 3404−3414.
66. Shinkai, A., Akita, M., Matsuyama, S., and Mizushima, S. (1990) *Biochem. Biophys. Res. Commun. 172*, 1217−1223.
67. Myers, J. K., Pace, C. N., and Scholtz, J. M. (1995) *Protein Sci. 4*, 2138−2148.
68. Stewart, R. C., VanBruggen, R., Ellefson, D. D., and Wolfe, A. J. (1998) *Biochemistry 37*, 12269−12279.
69. Ward, D. G., and Cavieres, J. D. (1998) *J. Biol. Chem. 273*, 33759−33765.
70. Beasty, A. M., Hurle, M., Manz, J. T., and Matthews, C. R. (1987) *Mutagenesis as a probe of protein folding and stability*, Vol. 1, Alan R. Liss, Inc., New York.
71. Finn, B. E., Chen, X., Jennings, P. A., Saal'au-Bethell, S. M., and Matthews, C. R. (1992) *Principles of protein stability. Part 1—reversible unfolding of proteins: kinetic and thermodynamic analysis*, Oxford University Press, Oxford, England.
72. Tanford, C. (1970) *Adv. Protein Chem. 24*, 1−95.
73. Shilton, B., Svergun, D. I., Volkov, V. V., Koch, M. H. J., Cusack, S., and Economou, A. (1998) *FEBS Lett. 436*, 277−282.
74. Willaert, K., Lowenthal, R., Sancho, J., Froeyen, M., Fersht, A., and Engelborghs, Y. (1992) *Biochemistry 31*, 711−716.
75. Smith, C. K., Bu, Z., Anderson, K. S., Sturtevant, J. M., Engelman, D. M., and Regan, L. (1996) *Protein Sci. 5*, 2009−2019.
76. Clark, A. C., Raso, S. W., Sinclair, J. F., Ziegler, M. M., Chaffotte, A. F., and Baldwin, T. O. (1997) *Biochemistry 36*, 1891−1899.
77. Grimsley, J. K., Scholtz, J. M., Pace, C. N., and Wild, J. R. (1997) *Biochemistry 36*, 14366−14374.
78. Fan, Y.-X., Zhou, J.-M., Kihara, H., and Tsou, C.-L. (1998) *Protein Sci. 7*, 2631−2641.
79. Hartl, F. U. (1996) *Nature 381*, 571−580.
80. Braig, K., Otwinowski, Z., Hegde, R., Boisvert, D. C., Joachimiak, A., Horwich, A. L., and Sigler, P. B. (1994) *Nature 371*, 578−586.
81. Bochkareva, E. S., Solovieva, M. E., and Girshovich, A. S. (1998) *Proc. Natl. Acad. Sci. U.S.A. 95*, 478−483.
82. Kimura, E., Akita, M., Matsuyama, S., and Mizushima, S. (1991) *J. Biol. Chem. 266*, 6600−6606.

BI000299Y